Propulsion and Power Research 2013;2(4):254–262

http://ppr.buaa.edu.cn/

Propulsion and Power Research

www.sciencedirect.com

ORGINAL ARTICLE

# Non-Newtonian fluid flow in an axisymmetric channel with porous wall

M. Hosseini[a,*], Z. Sheikholeslami[b], D.D. Ganji[c]

[a]*Department of Mechanical Engineering, Islamic Azad University, Qaemshahr Branch, Qaemshahr, Mazandaran, Iran*
[b]*Department of Civil Engineering, University of Mazandaran, Babolsar, Iran*
[c]*Department of Mechanical Engineering, Babol University of Technology, Babol, Iran*

Received 13 August 2013; accepted 14 October 2013
Available online 9 December 2013

**KEYWORDS**

Non-Newtonian fluid;
Axisymmetric channel;
Porous media;
Optimal Homotopy Asymptotic Method (OHAM);
Heat transfer

**Abstract** In the present article Optimal Homotopy Asymptotic Method (OHAM) is used to obtain the solutions of momentum and heat transfer equations of non-Newtonian fluid flow in an axisymmetric channel with porous wall for turbine cooling applications. Numerical method is used for validity of this analytical method and excellent agreement is observed between the solutions obtained from OHAM and numerical results. Trusting to this validity, effects of some other parameters are discussed. The results show that Nusselt number increases with increase of Reynolds number, Prandtl number and power law index.


## 1. Introduction

The problem of non-Newtonian fluid flow has been under a lot of attention in recent years because of its various applications in different fields of engineering specially the interest in heat transfer problems of non-Newtonian fluid flow, such as hot rolling, lubrication, cooling problems and drag reduction. Deburge and Han [1] studied a problem concerning heat transfer in channel flow. Natural convection of a non-Newtonian copper-water nanofluid was investigated by Domairry et al. [2]. They conclude that as the nanoparticle volume fraction increases, the momentum boundary layer thickness increases, whereas the thermal boundary layer thickness decreases. Sheikholeslami et al. [3] studied the problem of natural convection between a circular enclosure and a sinusoidal cylinder. They concluded that streamlines, isotherms, and the number, size and formation of the cells inside the enclosure strongly depend on the Rayleigh number, values of amplitude and the

*Corresponding author.
E-mail addresses: m.Hosseini545454@gmail.com (M. Hosseini), z_sh.eslami@yahoo.com (Z. Sheikholeslami).

Peer review under responsibility of National Laboratory for Aeronautics and Astronautics, China.

ELSEVIER Production and hosting by Elsevier

2212-540X 
http://dx.doi.org/10.1016/j.jppr.2013.10.001

## Nomenclature

| | |
|---|---|
| $\boldsymbol{A}$, $\boldsymbol{B}$ | symmetric kinematic matrices |
| $C$ | specific heat |
| $C_n$ | blade-wall temperature coefficients |
| $\delta v_m/\delta x_n$ | velocity gardients |
| $\delta a_m/\delta x_n$ | acceleration gradients |
| $x_k$ | general coordinates |
| $f$ | velocity function |
| $\bar{k}$ | fluid thermal conductivity |
| $n$ | power law index in temperature distribution |
| $Re$ | injection Reynolds number |
| $K_r$ | rotation parameter |
| $p$ | fluid pressure |
| $Pr$ | Prandtl number |
| $T$ | temperature |
| $q_n(\eta)$ | temperature function |
| $V$ | injection velocity |
| $u_r$ , $u_z$ | velocity components in $r$, $z$ directions, respectively |

*Greek letters*

| | |
|---|---|
| $\phi_k$ | viscosity coefficients |
| $\varphi$ | dissipation function |
| $\eta$ | dimension less coordinates in$z$direction |
| $\rho$ | fluid density |
| $\tau_{ij}$ | stress tensor component |
| $\psi$ | stream function |

number of undulations of the enclosure. Sheikholeslami et al. [4] performed a numerical study to investigate natural convection in a square cavity with curve boundaries filled with Cu-water nanofluid. Their results proved that the change of inclination angle has a significant impact on the thermal and hydrodynamic flow fields. Recently several authors investigated about natural convection heat transfer [5–22].

In the heart of all different engineering sciences, everything shows itself in the mathematical relation that most of these problems and phenomena are modeled by ordinary or partial differential equations. In most cases, scientific problems are inherently of nonlinearity that does not admit analytical solution, so these equations should be solved using special techniques. Some of them are solved using numerical techniques [23] and some are solved using the analytical method of perturbation [24]. In the numerical method, stability and convergence should be considered so as to avoid divergence or inappropriate results. In the analytical perturbation method, the small parameter is exerted to the equation. Since there are some limitations with the common perturbation method, and also because the basis of the common perturbation method is upon the existence of a small parameter, developing the method for different applications is very difficult. Therefore, some different methods have recently introduced some ways to eliminate the small parameter, such as the Homotopy Perturbation Method [25–27], Differential Transformation Method [28] and Homotopy Analysis Method [29] and some researchers applied these methods for engineering problems [30–32]. Optimal Homotopy Asymptotic Method (OHAM) is the other method and stronger method for solving nonlinear problems without depending to the small parameter. This method is developed and examined by some authors [33–35].

In this study, OHAM is applied to find the approximate solutions of nonlinear differential equations governing non-Newtonian fluid flow in an axisymmetric channel with a porous wall for turbine cooling applications and have made a comparison with the numerical solution. Results are given for the velocity and temperature for various values of Reynolds number, Prandtl number and power law index.

## 2. Mathematical formulation

### 2.1. Flow analysis

This study is concerned with simultaneous development of flow and heat transfer for non-Newtonian viscoelastic fluid flow on the turbine disc for cooling purposes. The problem to be considered is depicted schematically in Figure 1. The $r$-axis is parallel to the surface of disk and the $z$-axis is normal to it. The porous disc of the channel is at $z=+L$. The wall that coincides with the $r$-axis is heated externally and from the other perforated wall non-Newtonian fluid is injected uniformly in order to cool the heated wall.

As can observed in Figure 1 the cooling problem of the disk can be considered as a stagnation point flow with injection. For a steady, ax symmetric, non-Newtonian fluid flow the following equations can be written in cylindrical coordinates.

The continuity equation:

$$\frac{\partial(ru_r)}{\partial r}+\frac{\partial(ru_z)}{\partial z}=0 \tag{1}$$

And the momentum equations:

$$u_r\frac{\partial(u_r)}{\partial r}+u_z\frac{\partial(u_r)}{\partial z} = -\frac{1}{\rho}\frac{\partial P}{\partial r}+\frac{1}{\rho}\left[\frac{\partial\tau_{rr}}{\partial r}+\frac{1}{r}(\tau_{rr}-\tau_{\theta\theta})+\frac{\partial\tau_{rz}}{\partial z}\right] \tag{2}$$

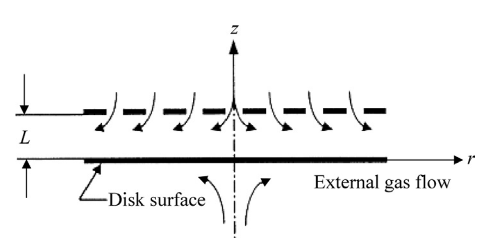


**Figure 1** Schematic diagram of the physical system.

$$u_r\frac{\partial(u_z)}{\partial r}+u_z\frac{\partial(u_z)}{\partial z}= -\frac{1}{\rho}\frac{\partial P}{\partial z}+\frac{1}{\rho}\left[\frac{\partial\tau_{zr}}{\partial r}+\frac{1}{r}\tau_{rz}+\frac{\partial\tau_{zz}}{\partial z}\right] \tag{3}$$

Here $\tau_{rr},\tau_{rz},\tau_{zr},\tau_{zz}$ are the components of stress matrix. The analytical model under consideration leads to the following boundary conditions:

$$@z=0 \qquad u_r=u_z=0 \tag{4}$$

$$@z=L \qquad u_r=0,\ \ u_z=-V \tag{5}$$

Here $u_r, u_z$ are the velocity components in the $r$ and $z$ directions and $V$ is the injection velocity; $\rho, P$ are the density, pressure. For particular class of viscoelastic and viscoinelastic fluids Rivlin [36] showed that if the stress components $\tau_{ij}$ at a point $x_k(k=1,2,3)$ and time $t$ are assumed to be polynominals in the velocity gradient $\frac{\delta v_m}{\delta x_n}$ $(m,n=1,2,3)$ and the acceleration gradients $\frac{\delta a_m}{\delta x_n}$ $(m,n=1,2,3)$, and if in addition the medium is assumed to be isontropic the stress matrix can be expressed in the form

$$\|\tau_{ij}\|=\phi_0\boldsymbol{I}+\phi_1\boldsymbol{A}+\phi_2\boldsymbol{B}+\phi_3\boldsymbol{A}^2+\dots \tag{6}$$

Here $\boldsymbol{I}$ is the unit matrices, $\boldsymbol{A}$ and $\boldsymbol{B}$ are symmetric kinematic matrixes defined by:

$$\boldsymbol{A}=\left\|\frac{\delta v_i}{\delta x_j}+\frac{\delta v_j}{\delta x_i}\right\|,\qquad \boldsymbol{B}=\left\|\frac{\delta a_i}{\delta x_j}+\frac{\delta a_j}{\delta x_i}+2\frac{\delta v_m}{\delta x_i}\frac{\delta v_m}{\delta x_j}\right\| \tag{7}$$

And $\phi_k(k=0,1,2,3)$ are polynomials in the invariants of $\boldsymbol{A}$, $\boldsymbol{B}$, $\boldsymbol{A}^2$. This study is restricted to second order fluids for which $\phi_k(k=0,1,2,3)$ are constant and $\phi_k(k=4,5,\dots)$ are zero. So that the stress components are as follows:

$$\tau_{rr}=\phi_1A_{rr}+\phi_2{A_{rr}}^2+\phi_3B_{rr} \tag{8}$$

$$\tau_{zz}=\phi_1A_{zz}+\phi_2{A_{zz}}^2+\phi_3B_{zz} \tag{9}$$

$$\tau_{\theta\theta}=\phi_1A_{\theta\theta}+\phi_2{A_{\theta\theta}}^2+\phi_3B_{\theta\theta} \tag{10}$$

$$\tau_{rz}=\phi_1A_{rz}+\phi_2{A_{rz}}^2+\phi_3B_{rz} \tag{11}$$

For the solution of the problem depicted in Figure 1 in the case of axially symmetric flow it is convenient to define a stream function so that the continuity equation is satisfied:

$$\psi=Vr^2f(\eta) \tag{12}$$

where $\eta=z/L$ and the velocity components can be derived as:

$$u_r=\frac{Vr}{L}f'(\eta) \tag{13}$$

$$u_z=-2Vf(\eta) \tag{14}$$

Using Eqs. (12)–(14) the equations of motion reduce to:

$$f'^2-2ff''=-\frac{L^2}{\rho V^2 r}\frac{\partial P}{\partial r}+\frac{\phi_1}{\rho VL}f''' +\frac{\phi_2}{\rho L^2}(f''^2-2f'f''')+\frac{\phi_3}{\rho L^2}(f''^2-2ff^{iv}) \tag{15}$$

$$4ff'=-\frac{L^2}{\rho V^2}\frac{\partial P}{\partial z}-2\frac{\phi_1}{\rho VL}f'' +2\frac{\phi_2}{\rho L^2}\left(14f'f''+\frac{r^2}{L}f''f'''\right) +4\frac{\phi_3}{\rho L^2}\left(11f'f''+ff'''+\frac{r^2}{L}f'f'''\right) \tag{16}$$

The pressure term can be eliminated by differentiating Eq. (15) with respect to $z$ and Eq. (16) with respect to $r$ and subtracting the resulting equations. This gives the following equations:

$$-2ff'''=\frac{f^{iv}}{Re}-K_1\,(4f''f'''+2f'f^{iv}) -K_2\,(4f''f'''+2f'f^{iv}+2ff^{v}) \tag{17}$$

where $K_1=\frac{\Phi_2}{\rho L^2}$, $K_2=\frac{\Phi_3}{\rho L^2}$ is the injection Reynolds number.

For $K_2=0$, the equation turned to:

$$f^{iv}+2Re\,ff'''-K_1\,Re\,(4f''f'''+2f'f^{iv})=0 \tag{18}$$

The boundary conditions are:

$$f(0)=0,\quad f'(0)=0,\qquad f(1)=1,\quad f'(1)=0. \tag{19}$$

### 2.2. Heat transfer analysis

The energy equation for the present problem with viscous dissipation in non-dimensional form is given:

$$\rho C\left(u_r\frac{\partial T}{\partial r}+u_z\frac{\partial T}{\partial z}\right)=\bar{k}\nabla^2T+\varphi \tag{20}$$

$$\varphi=\tau_{rr}\frac{\partial u_r}{\partial r}+\tau_{\theta\theta}\frac{u_r}{r}+\tau_{zz}\frac{\partial u_z}{\partial z}+\tau_{rz}\left(\frac{\partial u_r}{\partial z}+\frac{\partial u_z}{\partial r}\right) \tag{21}$$

Here $u_r, u_z$ are the velocity components in the $r$ and $z$ directions and $V$ is the injection velocity; $\rho, P, T, C, \bar{k}$ are the density, pressure, temperature, specific heat, and heat conduction coefficient of fluid, respectively. $\varphi$ is the dissipation function.

Letting the blade wall ($z=0$) temperature distribution be $T_w = T_0 + \sum_{n=0}^{\infty} C_n\,(r/L)^n$

And assuming the fluid temperature to have the form of [1]

$$T = T_0 + \sum_{n=0}^{\infty} C_n \left(\frac{r}{L}\right)^n q_n(\eta) \tag{22}$$

where $T_0$ is the temperature of the incoming coolant ($z=L$) and neglecting dissipation effect the following equations and boundary conditions are obtained:

$$q_n'' - Pr\,Re(f' q_n - 2f q_n') = 0, \quad (n = 0, 2, 3, 4, \ldots) \tag{23}$$

$$q_n(0) = 1, \quad q_n(1) = 0. \tag{24}$$

## 3. Fundamentals of Optimal Homotopy Asymptotic Method

Following differential equation is considered:

$$L(u(t)) + N(u(t)) + g(t) = 0, \quad B(u) = 0 \tag{25}$$

where $L$ is a linear operator, $\tau$ is an independent variable, $u(t)$ is an unknown function, $g(t)$ is a known function, $N(u(t))$ is a nonlinear operator and $B$ is a boundary operator. By means of OHAM one first constructs a set of equations:

$$\begin{aligned}&(1-p)[L(\phi(\tau,p)) + g(\tau)] - H(p)[L(\phi(\tau,p))\\ &\quad + g(\tau) + N(\phi(\tau,p))] = 0\\ &B(\phi(\tau,p)) = 0,\end{aligned} \tag{26}$$

where $p \in [0,1]$ is an embedding parameter, $H(p)$ denotes a nonzero auxiliary function for $p \neq 0$ and $H(0) = 0$, $\phi(\tau,p)$ is an unknown function. Obviously, when $p = 0$ and $p = 1$, it holds that:

$$\phi\,(\tau,0) = u_0(\tau), \quad \phi\,(\tau,1) = u(\tau). \tag{27}$$

Thus, as $p$ increases from 0 to 1, the solution $\phi\,(\tau,p)$ varies from $u_0(\tau)$ to the solution $u(\tau)$, where $u_0(\tau)$ is obtained from Eq. (2) for $p = 0$:

$$\begin{aligned}&L(u_0(\tau)) + g(\tau) = 0,\\ &B(u_0) = 0.\end{aligned} \tag{28}$$

We choose the auxiliary function $H(p)$ in the form:

$$H(p) = pC_1 + p_2 C_2 + \ldots \tag{29}$$

where $C_1, C_2, \ldots$ are constants which can be determined later.

Expanding $\phi(\tau,p)$ in a series with respect to $p$, one has:

$$\phi(\tau,p,C_i) = u_0(\tau) + \sum_{k\geq 1} u_k(\tau,C_i)p_k, \quad i = 1,2,\ldots \tag{30}$$

Substituting Eq. (30) into Eq. (26), collecting the same powers of $p$, and equating each coefficient of $p$ to zero, we obtain set of differential equation with boundary conditions. Solving differential equations by boundary conditions $u_0(\tau)$, $u_1(\tau,C_1)$, $u_2(\tau,C_2)$, … are obtained. Generally speaking, the solution of Eq. (1) can be determined approximately in the form:

$$\tilde{u}^{(m)} = u_0(\tau) + \sum_{k=1}^{m} u_k(\tau,C_i). \tag{31}$$

Note that the last coefficient $C_m$ can be function of $\tau$. Substituting Eq. (31) into Eq. (25), there results the following residual:

$$R(\tau,C_i) = L(\tilde{u}^{(m)}(\tau,C_i)) + g(\tau) + N(\tilde{u}^{(m)}(\tau,C_i)). \tag{32}$$

If $R(\tau,C_i) = 0$ then $\tilde{u}^{(m)}(\tau,C_i)$ happens to be the exact solution. Generally such a case will not arise for nonlinear problems, but we can minimize the functional:

$$J(C_1,C_2,\ldots,C_n) = \int_a^b R^2(\tau,C_1,C_2,\ldots,C_m)\,d\tau, \tag{33}$$

where $a$ and $b$ are two values, depending on the given problem. The unknown constants $C_i (i = 1,2,\ldots,m)$ can be identified from the conditions:

$$\frac{\partial J}{\partial C_1} = \frac{\partial J}{\partial C_2} = \ldots = 0. \tag{34}$$

With these constants, the approximate solution (of order $m$) (Eq. (31)) is well determined. It can be observed that the method proposed in this work generalizes these two methods using the special (more general) auxiliary function $H(p)$.

## 4. Solution with Optimal Homotopy Asymptotic Method

In this section, OHAM is applied to nonlinear ordinary differential Eqs. (18) and (23). According to the OHAM, applying Eqs. (26) to (18) and (23):

$$\begin{aligned}&f^{iv} + 2Reff''' - K_1 Re(4f''f''' + 2f'f^{iv}) = 0,\\ &q_n'' - Pr\,Re(f' q_n - 2f q_n') = 0,\\ &(n = 0, 2, 3, 4, \ldots)\end{aligned} \tag{35}$$

where primes denote differentiation with respect to $\eta$. We consider $f$, $q_n$, $H_1(p)$ and $H_2(p)$ as following:

$$\begin{aligned}&f = f_0 + pf_1 + p^2 f_2,\\ &q_n = q_{n_0} + pq_{n_1} + p^2 q_{n_2},\\ &H_1(p) = pC_{11} + p^2 C_{12},\\ &H_2(p) = pC_{21} + p^2 C_{22}.\end{aligned} \tag{36}$$

Substituting $f$, $q_n$, $H_1(p)$ and $H_2(p)$ from Eq. (36) into Eq. (35) and some simplification and rearranging based on powers of $p$-terms, we have:

$$p^0: \quad f^{IV}=0,$$
$$q_n''=0,$$
$$f_0(0)=0,\ f_0'(0)=0,$$
$$f_0(1)=1,\ f_0'(1)=0. \tag{37}$$
$$q_{n_0}(0)=1,\ q_{n_0}(1)=0.$$

$$p^1: \quad f_1^{IV}+C_{11}f_0^{IV}+2C_{11}\,Re\,f_0f_0'''$$
$$-4C_{11}\,K_1Re\,f_0''f_0'''$$
$$-2C_{11}\,K_1Re\,f_0^{IV}f_0'-f_0^{IV}=0,$$
$$2\,C_{21}\,Re\ \ Pr\,q_{n_0}'$$
$$-C_{21}\,Re\ \ Pr\,n\,f_0'\,q_{n_0}+q_{n_1}''$$
$$+C_{21}\,q_{n_0}''-q_{n_0}''=0, \tag{38}$$
$$f_1(0)=0,\quad f_1'(0)=0,$$
$$f_1(1)=0,\quad f_1'(1)=0.$$
$$q_{n_1}(0)=0,\quad q_{n_1}(1)=0,$$
$$\vdots$$

Solving Eqs. (37) and (38) with boundary conditions:

$$f_0(\eta)=-2\eta^3+3\eta^2,$$
$$q_{n_0}(\eta)=-\eta+1, \tag{39}$$

$$f_1(\eta)=C_{11}\,Re(-0.05714285714\eta^7+0.2\eta^6$$
$$+4.8n\eta^5-12n\eta^4-0.5142857144\eta^3$$
$$+9.6n\eta^3),$$
$$q_{n_1}(\eta)=C_{21}\,Pr\,Re(0.3n\eta^5-n\eta^4+n\eta^3$$
$$+\eta^2-0.3n\eta-\eta),$$
$$\vdots \tag{40}$$

The terms $f_2(\eta)$ and $q_{n_2}(\eta)$ are mentioned graphically because they are too long. Therefore final expression for $f(\eta)$ and $q_n(\eta)$ are:

$$f(\eta)=f_0(\eta)+f_1(\eta)+f_2(\eta),$$
$$q_n(\eta)=q_{n_0}(\eta)+q_{n_1}(\eta)\ +q_{n_2}(\eta). \tag{41}$$

From Eq. (32) by Substituting $f(\eta)$ and $q_n(\eta)$ into Eq. (41), $R_1(\eta,C_{11},C_{12})$ and $R_2(\eta,C_{21},C_{22})$ are obtained and $J_1$ and $J_2$ are obtained in the flowing manner:

$$J_1(C_{11},C_{12})=\int_0^\infty R_1{}^2(\eta,C_{11},C_{12})\,\mathrm{d}\eta,$$
$$J_2(C_{21},C_{22})=\int_0^\infty R_2{}^2(\eta,C_{21},C_{22})\,\mathrm{d}\eta.$$

The constants $C_{11},\ C_{12},C_{21}$ and $C_{22}$ obtain from Eq. (42). In the particular cases:

$Pr=1,K_1=0.01,n=0$ and $Re=0.5$

$$C_{11}=1.09935,C_{12}=-0.0167296,$$
$$C_{21}=1.08018,C_{22}=-0.0572104. \tag{42}$$

By substituting Eqs. (42) into (41), an expression for $f(\eta)$ and $q_n(\eta)$ are obtained.

## 5. Results and discussion

The objective of the present study is to apply Optimal Homotopy Asymptotic Method to obtain an explicit analytic solution of heat transfer equation of a non-Newtonian fluid flow in an axisymmetric channel with a porous wall for turbine cooling applications (Figure 1).

Validity of Optimal Homotopy Asymptotic Method is shown in Table 1 and Figure 2. Excellent agreement between numerical solution obtained by four-order Rung-Kutte method and analytical solution is obvious in Table 1 and this figure too. In Table 1, error is introduced as follows: Error $=|f(\eta)_{\mathrm{NM}}-f(\eta)_{\mathrm{OHAM}}|$.

This accuracy gives high confidence to us about validity of this problem and reveals an excellent agreement of engineering accuracy. This investigation is completed by depicting the effects of some important parameters to evaluate how these parameters influence on this fluid. The velocities $f(\eta)$ and $f'(\eta)$, and temperature $q_n(\eta)$ profiles for various parameters $Re$, $Pr$, $K_1$ and $n$ are illustrated in Figures 3–5.

As seem in Figure 3 for constant value of $K_1$ velocity profile increases as Reynolds number increases. At low Reynolds numbers the velocity profile exhibit center line symmetry indicating a poisuille flow for non-Newtonian fluids. At higher Reynolds numbers the maximum velocity point is shift to the solid wall where shear stress becomes larger as the Reynolds number grows. Since $f''(0)$ is measure of friction force, it is advisable to use viscoinelastic fluids as a coolant fluid at least for industrial gas turbine engines. Figure 4 shows the variation $f''(0)$ for different

**Table 1** Comparison between numerical results and OHAM solution at $Re=0.5,\quad K_1=0.01,\quad Pr=1,\quad n=0.$

| $\eta$ | $f$ | $q_n$ |
|---|---|---|
| | Error | Error |
| 0 | 0 | 0 |
| 0.1 | 0.0000053 | 0.00000014 |
| 0.2 | 0.0000091 | 0.00000013 |
| 0.3 | 0.0000104 | 0.00000011 |
| 0.4 | 0.0000090 | 0.0000005 |
| 0.5 | 0.0000058 | 0.0000017 |
| 0.6 | 0.0000021 | 0.0000036 |
| 0.7 | 0.00000045 | 0.0000052 |
| 0.8 | 0.0000012 | 0.0000052 |
| 0.9 | 0.00000057 | 0.0000026 |
| 1 | 0 | 0 |

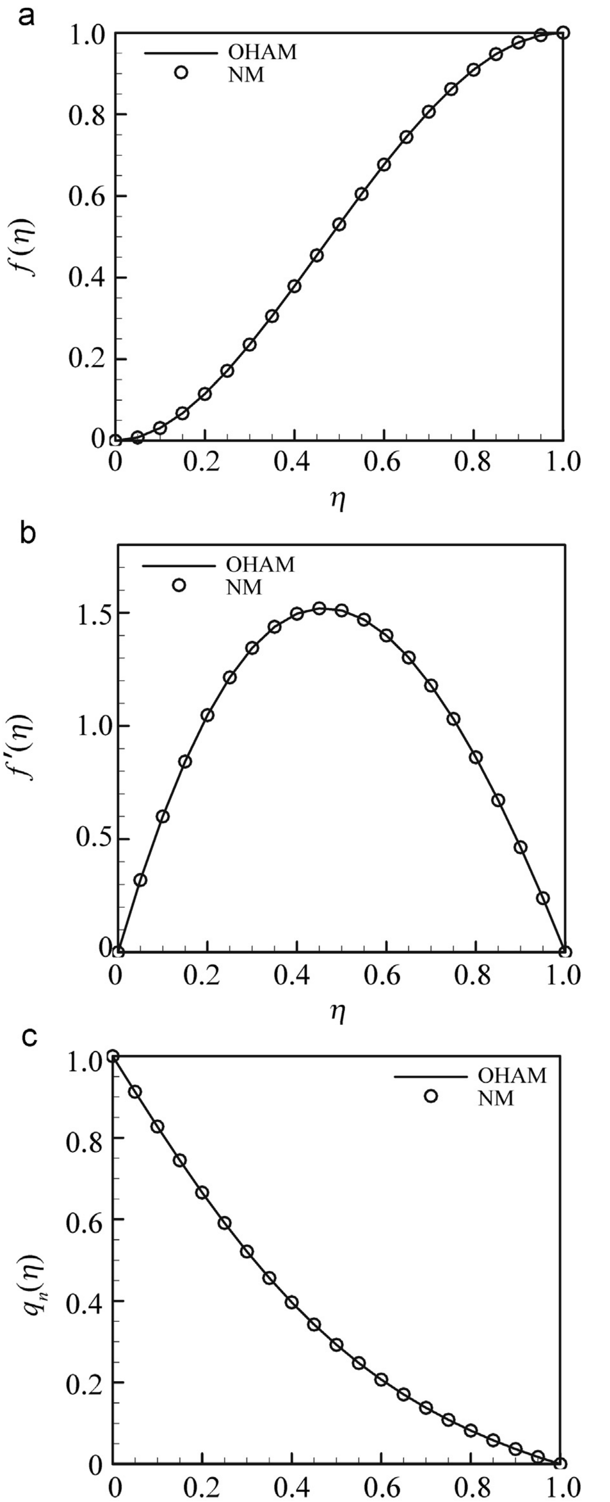


**Figure 2** Comparison between the solutions via OHAM and numerical solution for (a) $f(\eta)$, (b) $f^{'}(\eta)$ and (c) $q_n(\eta)$, when $K_1 = 0.01$, $Pr = 1$, $n = 2$ and $Re = 1$.

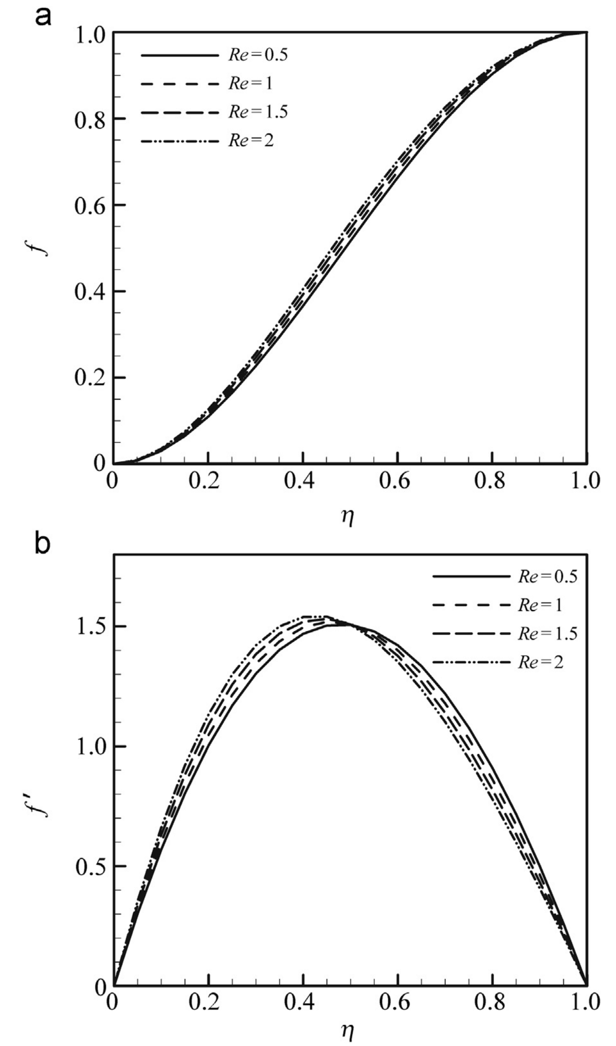


**Figure 3** Velocity component profile (a) $f$, (b) $f'$ for variable $Re$ at $K_1 = 0.01$.

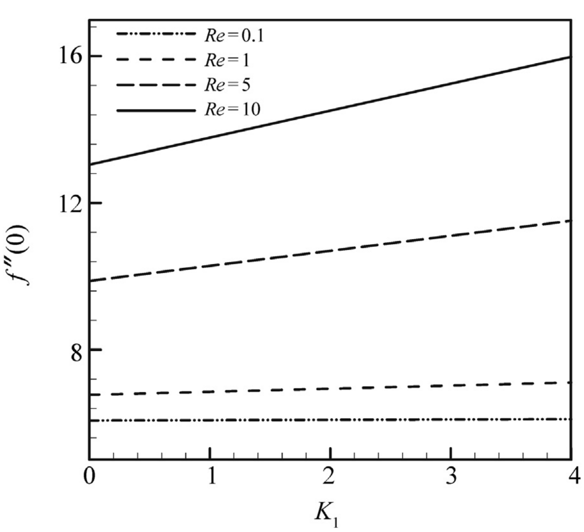


**Figure 4** Skin friction under the effect of $K_1$ and $Re$.

values of $K_1$ and Reynolds number. One can observe that for constant values of $K_1$, $f^{''}(0)$ increase with increase of value of $Re$, especially at high Reynolds numbers.

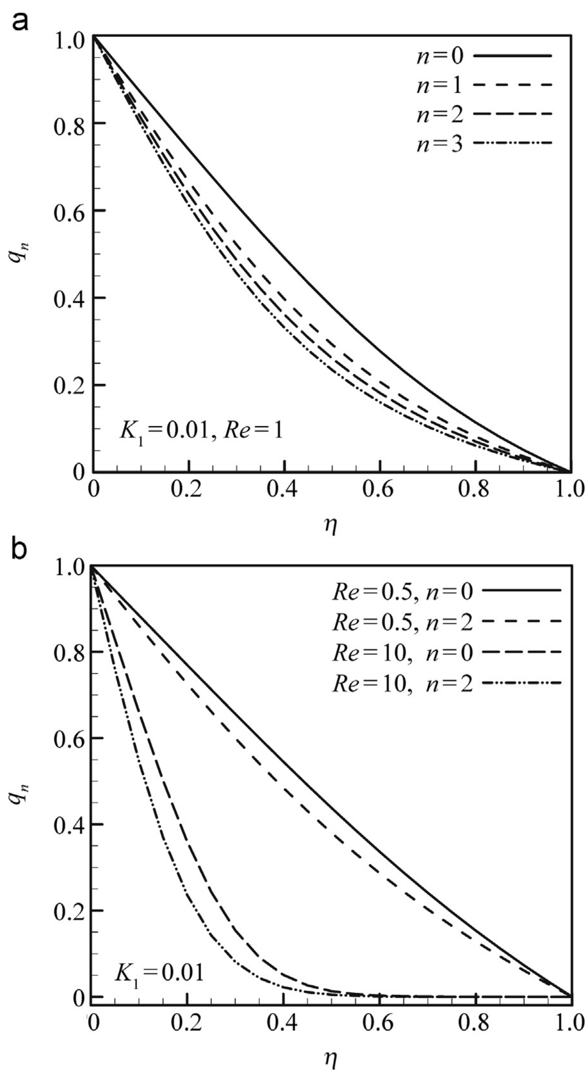


**Figure 5** Temperature profile ($q_n$) (a) for variable $n$ at $K_1 = 0.01$, $Re = 1$ and (b) at $K_1 = 0.01$.

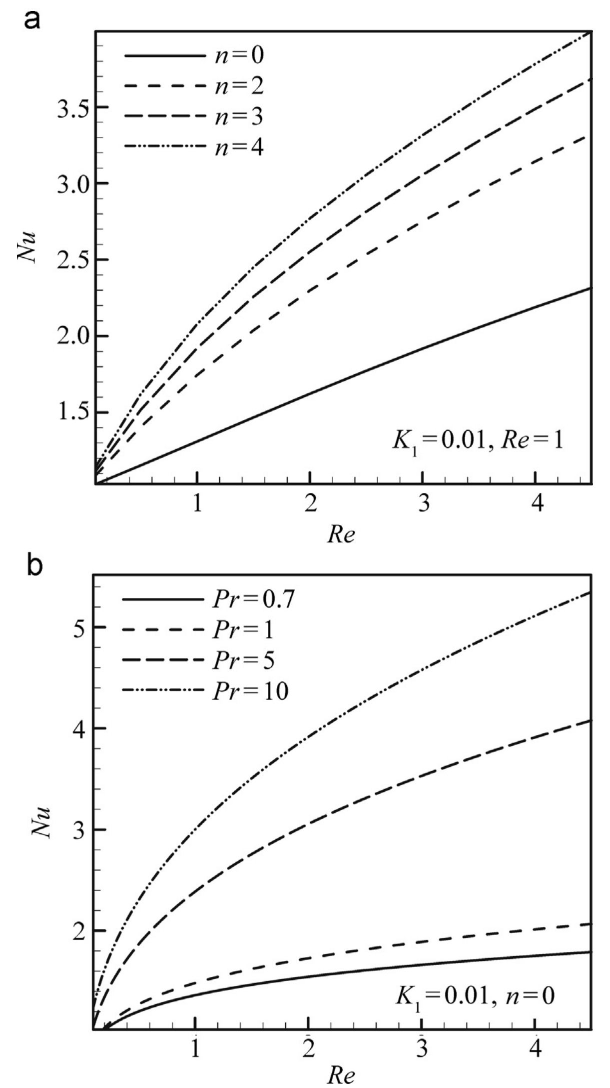


**Figure 6** Nusselt number (a) for variable $n$ at $K_1 = 0.01$, $Re = 1$ and (b) for variable $Re$ at $K_1 = 0.01$, $n = 0$.

In Figure 5 temperature profile for different values of power law index ($n$) and Reynolds number are shown. It shows that for constant value of $\eta$ temperature increases if power law index decreases. Also it shows that increasing Reynolds number leads to increase the curve of temperature profile and decrease of $q_n(\eta)$ values. Figure 6 illustrates how Nusselt number ($Nu = -q_n'(0)$) can be changed with various amount of $Re$, $Pr$, $n$. It shows that Nusselt number increases with increase of Reynolds number, Prandtl number and power law index.

## 6. Conclusion

In this paper, OHAM is applied to solve the problem of non-Newtonian fluid flow in an axisymmetric channel with a porous wall for turbine cooling applications. Complementary numerical solutions were obtained via fourth grade order Rung-Kutta and very excellent agreement between the solutions obtained from OHAM. The results show that the increment in the Reynolds number has similar effects on velocity components, both of them increases with increase of Reynolds number. At higher Reynolds numbers the maximum velocity point is shift to the solid wall where shear stress becomes larger as the Reynolds number grows. Increment in skin friction is the effect of Reynolds number increment, especially at high Reynolds numbers. Increasing Reynolds number, Prandtl number and power law index leads to increase in Nusselt number.

## References

[1] L.L. Debruge, L.S. Han, Heat transfer in a channel with a porous wall for turbine cooling application, ASME Journal of Heat Transfer 94 (4) (1972) 385–390.

[2] D. Domairry, M. Sheikholeslami, H.R. Ashorynejad, R.S.R. Gorla, M. Khani, Natural convection flow of a non-Newtonian nanofluid between two vertical flat plates,

Proceedings of the Institution of Mechanical Engineers, Part N: Journal of Nanoengineering and Nanosystems 225 (3) (2012) 115–122, http://dx.doi.org/10.1177/1740349911433468.
[3] M. Sheikholeslami, M. Gorji-Bandpy, I. Pop, Soheil Soleimani, Numerical study of natural convection between a circular enclosure and a sinusoidal cylinder using control volume based finite element method, International Journal of Thermal Sciences 72 (2013) 147–158.
[4] M. Sheikholeslami, M. Gorji-Bandpy, S.M. Seyyedi, D.D. Ganji, H.B. Rokni, S. Soleimani, Application of LBM in simulation of natural convection in a nanofluid filled square cavity with curve boundaries, Powder Technology 247 (2013) 87–94.
[5] M. Sheikholeslami, M. Gorji-Bandpy, S. Soleimani, Two phase simulation of nanofluid flow and heat transfer using heatline analysis, International Communications in Heat and Mass Transfer 47 (2013) 73–81.
[6] M. Sheikholeslami, M. Gorji-Bandpy, D.D. Ganji, Numerical investigation of MHD effects on Al2O3-water nanofluid flow and heat transfer in a semi-annulus enclosure using LBM, Energy 60 (2013) 501–510.
[7] M. Sheikholeslami, M. Gorji-Bandpy, R. Ellahi, M. Hassan, S. Soleimani, Effects of MHD on Cu-water nanofluid flow and heat transfer by means of CVFEM, Journal of Magnetism and Magnetic Materials 349 (2014) 188–200.
[8] M. Sheikholeslami, M. Gorji-Bandpy, D.D. Ganji, Natural convection in a nanofluid filled concentric annulus between an outer square cylinder and an inner elliptic cylinder, Scientia Iranica, Transaction B: Mechanical Engineering 20 (4) (2013) 1–13.
[9] M. Sheikholeslami, M. Hatami, D.D. Ganji, Analytical investigation of MHD nanofluid flow in a Semi-Porous Channel, Powder Technology 246 (2013) 327–336.
[10] M. Sheikholeslami, M. Gorji-Bandpy, D.D. Ganji, S. Soleimani, Natural convection heat transfer in a cavity with sinusoidal wall filled with CuO-water nanofluid in presence of magnetic field, Journal of the Taiwan Institute of Chemical Engineers, http://dx.doi.org/10.1016/j.jtice.2013.04.019.
[11] M. Sheikholeslami, M. Gorji-Bandpy, G. Domairry, Free convection of nanofluid filled enclosure using lattice Boltzmann method (LBM), Applied Mathematics and Mechanics 34 (7) (2013) 1–15.
[12] M. Sheikholeslami, M. Gorji-Bandpy, D.D. Ganji, S. Soleimani, Effect of a magnetic field on natural convection in an inclined half-annulus enclosure filled with Cu-water nanofluid using CVFEM, Advanced Powder Technology, http://dx.doi.org/10.1016/j.apt.2013.01.012.
[13] M. Sheikholeslami, M. Gorji-Bandpy, D.D. Ganji, S. Soleimani, MHD natural convection in a nanofluid filled inclined enclosure with sinusoidal wall using CVFEM, Neural Comput & Applic, http://dx.doi.org/10.1007/s00521-012-1316-4.
[14] M. Sheikholeslami, M. Gorji-Bandpy, D.D. Ganji, S. Soleimani, S.M. Seyyedi, Natural convection of nanofluids in an enclosure between a circular and a sinusoidal cylinder in the presence of magnetic field, International Communications in Heat and Mass Transfer 39 (2012) 1435–1443.
[15] S. Soleimani, M. Sheikholeslami, D.D. Ganji, M. Gorji-Bandpay, Natural convection heat transfer in a nanofluid filled semi-annulus enclosure, International Communications in Heat and Mass Transfer 39 (2012) 565–574.
[16] M. Sheikholeslami, M. Gorji-Bandpay, D.D. Ganji, Magnetic field effects on natural convection around a horizontal circular cylinder inside a square enclosure filled with nanofluid, International Communications in Heat and Mass Transfer 39 (2012) 978–986.
[17] D.D. Ganji, M. Gorji, M. Hatami, A. Hasanpour, N. Khademzadeh, Propulsion and launching analysis of variable-mass rockets by analytical methods, Propulsion and Power Research 2 (3) (2013) 225–233.
[18] S. Bhattrai, H. Tang, Comparative performance analysis of combined-cycle pulse detonation turbofan engines (PDTEs), Propulsion and Power Research 2 (3) (2013) 214–224.
[19] A. Elhefny, G.Z. Liang, Stress and deformation of rocket gas turbine disc under different loads using finite element modelling, Propulsion and Power Research 2 (1) (2013) 38–49.
[20] M. Sheikholeslami, M. Hatami, D.D. Ganji, Nanofluidflow and heat transfer in a rotating system in the presence of a magnetic-field, Journal of Molecular Liquids 190 (2014) 112–120.
[21] M.R. Reyhani, M. Alizadeh, A. Fathi, H. Khaledi, Turbine blade temperature calculation and life estimation - a sensitivity analysis, Propulsion and Power Research 2 (2) (2013) 148–161.
[22] M. Sheikholeslami, D.D. Ganji, M. Gorji-Bandpy, Soheil Soleimani, Magnetic field effect on nanofluid flow and heat transfer using KKL model, Journal of the Taiwan Institute of Chemical Engineers, http://dx.doi.org/10.1016/j.jtice.2013.09.018, in press
[23] P.S.V.N. Murthy, P. Singh, Thermal dispersion effects on non-Darcy natural convection over horizontal plate with surface mass flux, Archive of Applied Mechanics 67 (1997) 487–495.
[24] E. Magyari, B. Keller, Exact solutions for self-similar boundary-layer flows induced by permeable stretching walls, European Journal of Mechanics B-Fluids 19 (2000) 109–122.
[25] M. Sheikholeslami, D.D. Ganji, Heat transfer of Cu-water nanofluid flow between parallel plates, Powder Technology 235 (2013) 873–879.
[26] J.H. He, Homotopy perturbation method for bifurcation on nonlinear problems, International Journal of Non-linear Science and Numerical Simulation 6 (2005) 207–218.
[27] M. Sheikholeslami, H.R. Ashorynejad, D.D. Ganji, A. Kolahdooz, Investigation of rotating MHD viscous flow and heat transfer between stretching and porous surfaces using analytical method, Hindawi Publishing Corporation Mathematical Problems in Engineering Volume 2011 (2011), Article ID 258734, 17 pages, http://dx.doi.org/10.1155/2011/258734.
[28] I.H. Abdel-Halim Hassan, On solving some eigenvalue problems by using a differential transformation, Applied Mathematics and Computation 127 (1) (2002) 1–22.
[29] S.J. Liao, The proposed homotopy analysis technique for the solution of nonlinear problems, Ph.D. thesis, Shanghai Jiao Tong University, 1992.
[30] M. Sheikholeslami, F.B. Sheykholeslami, S. Khoshhal, H. Mola-Abasia, D.D. Ganji, H.B. Rokni, Effect of magnetic field on Cu-water nanofluid heat transfer using GMDH-type neural network, Neural Comput & Applic, http://dx.doi.org/10.1007/s00521-013-1459-y.
[31] A. Golbabai, D. Ahmadian, Homotopy pade method for solving linear and nonlinear integral equations, International Journal of Nonlinear Dynamics in Engineering and Sciences 1 (1) (2009) 59–66.
[32] A.A. Joneidi, G. Domairry, M. Babaelahi, M. Mozaffari, Analytical treatment on Magnetohydrodynamic (MHD) flow and heat transfer due to a stretching hollow cylinder, International Journal for Numerical Methods in Fluids, http://dx.doi.org/10.1002/fld.2087.

[33] V. Marinca, N. Herisanu, Application of optimal homotopy asymptotic method for solving nonlinear equations arising in heat transfer, International Communications in Heat and Mass Transfer 35 (2008) 710–715.

[34] M. Sheikholeslami, H. Reza Ashorynejad, Davood Domairry, Ishak Hashim, Investigation of the laminar viscous flow in a semi-porous channel in the presence of uniform magnetic field using optimal homotopy asymptotic method, Sains Malaysiana 41 (10) (2012) 1177–1229.

[35] V. Marinca, N. Herişanu, Optimal homotopy asymptotic method with application to thin film flow, Central European Journal of Physics 6 (2008) 1608–1644.

[36] R.S. Rivlin, Plane strain of a net formed by inextensible cords, J. Rational Mech. Anal 4 (1955) 323.